Settlement Estimation of Multiple Footings in Sands

J. Lee
Yonsei University, Seoul, South Korea
J. Eun
University of Texas at Austin, Austin, USA
M. Prezzi & R. Salgado
Purdue University, West Lafayette, USA

ABSTRACT: Shallow foundations are popular for various building structures and typically consist of multiple footings, often in close proximity. The most widely used methods for the estimation of footing settlement have been developed for an isolated footing and do not provide a way to account for interaction between adjacent footings. In this paper, a method of settlement estimation that takes account of the proximity of neighboring footing is presented based on Schmertmann's framework. Three-dimensional non-linear finite element analyses are performed to obtain the load-settlement responses and strain distributions in the foundation soils for multiple footings separated by different footing edge-to-edge distances. Various multiple footing configurations were considered in the finite element analyses.

1 INTRODUCTION

Footings are often used for foundations of various structures. The typical design procedure of a footing includes the assessment of limit bearing capacity and the estimation of settlement under working loads. In routine practice, the estimation of footing settlement in sands is commonly based on the linear-elastic approach using a representative elastic modulus. In the conventional approach for the footing settlement estimation, interactions between adjacent footings are not specifically taken into account. However, it is noted that shallow foundations for typical building structures consist of multiple footings, often in close proximity. The mechanical interaction between adjacent footings generates settlements greater than those for isolated footings, and therefore neglect of the interactions between adjacent footings may result in unconservative footing design.

Schmertmann's method is one of several methods (Meyerhof 1965, Schmertmann et al. 1978, Berardi et al. 1991) that base estimates of the settlement of footings in sand on results from in-situ field tests, such as the standard penetration test (SPT) or the cone penetration test (CPT). In Schmertmann's method, the strains are calculated using a strain influence factor and elastic modulus estimated from the CPT cone resistance q_c for the case of isolated footings. In this paper, following the framework of Schmertmann's method, the interaction effect of neighboring footings on settlement is investigated using the finite element analysis. For this purpose, non-linear finite element analyses are per-

formed for multiple footings separated by different footing distances. Based on results from the finite element analyses, strain influence factors for multiple footings are presented. Design equations of strain influence diagram parameters for multiple footing conditions are presented as well.

2 FOOTING SETTLEMENT CALCULATION USING CONE RESISTANCE

Schmertmann's method (Schmertmann 1970, Schmertmann et al. 1978) is essentially an elastic-based approach with modulus values obtained using q_c and strain influence factor I_z given in the form of the simplified diagram shown in Figure 1. Other parameters defining the diagram are the value I_{z0} of the strain influence factor at the footing base, its peak value I_{zp}, and the depths z_{fp} to I_{zp} and z_{f0} to the bottom of the diagram. The depth z_{f0} can be referred to as the strain influence depth. As shown in Figure 1, the diagram extends down to 2B and 4B, and the depth z_{fp} to I_{zp} is equal to 0.5B and B for square and strip footings, respectively.

For the implementation of the method, the soil on which the footing rests is divided in several layers based on the q_c profile, and, with depth and time factors included, the equation for the settlement calculation is given as follows:

$$s = C_1 C_2 (q_b - \sigma'_{v,z_f=0}) \sum \left(\frac{I_z \Delta z_i}{E_i} \right) \tag{1}$$

where C_1 and C_2 = depth and time factors; $\sigma'_{v,zf=0}$ = vertical effective stress at footing base level before the footing was constructed; I_{zi} = influence factor corresponding to each sublayer; Δz_i = thickness of each sublayer; E_i = representative elastic modulus of each sublayer. The elastic modulus E_i of each individual sublayer is obtained from the representative cone resistance q_{ci} for that sublayer. While E/q_c is typically taken constant in the conventional Schmertmann method, Lee & Salgado (2002) developed a E/q_c relationship in terms of the settlement level and the relative density D_R to account for the non-linearity of the soil stress-strain relationship as follows:

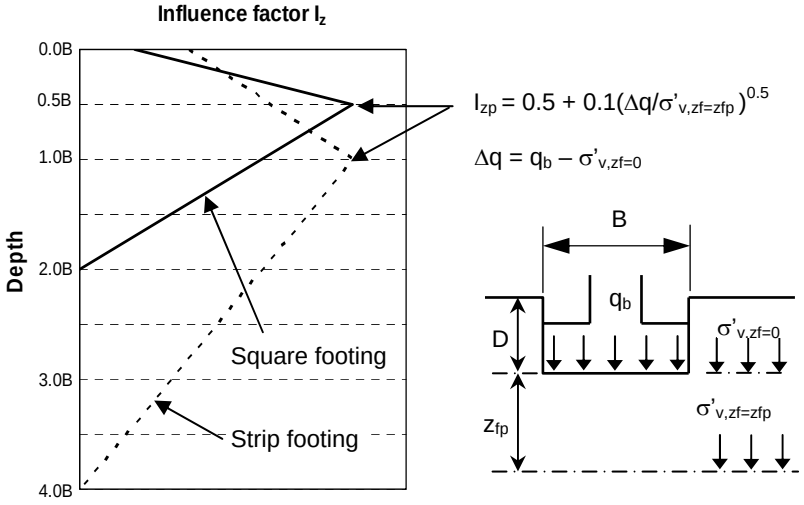

Figure 1. Strain influence diagram for Schmertmann's method.

$$\frac{E}{q_c} = 1.4 \cdot \left(\frac{s}{s_R}\right)^{-0.285} \left(\frac{B}{B_R}\right)^{0.4} \left(\frac{D_R}{100}\right)^{-0.65} \quad (2)$$

where s_R = reference settlement = 1 cm; s = settlement in the same unit as s_R; B_R = reference footing width = 1m; B = footing width in the same unit as the B_R; and D_R = relative density in %.

3 FINITE ELEMENT MODELING OF MULTIPLE FOOTINGS

3.1 *Soil model*

For the finite element analyses of axially loaded multiple footings, the non-linear stress-strain model of Lee & Salgado (1999) was employed. In this model, the elastic modulus is treated as a state-dependent variable and given as follows:

$$\frac{G}{G_o} = [1 - f(\frac{\sqrt{J_2} - \sqrt{J_{2o}}}{\sqrt{J_{2\max}} - \sqrt{J_{2o}}})^g](\frac{I_1}{I_{1o}})^{n_g} \quad (3)$$

where G = secant shear modulus; G_0 = small-strain shear modulus; J_2 , J_{20}, and J_{2max} = the current, initial, and maximum second invariants of the deviatoric stress tensor; I_1 and I_{10} are the first invariants of the stress tensor at the current and initial states; and f, g, and n_g = material parameters. Eq. (3) represents the non-linear degradation of the shear modulus from its initial maximum value G_0.

In order to consider the non-linear characteristics of shear strength for sands, a curved form of the Drucker-Prager failure criterion was adopted employing a state-dependent peak friction angle. For the peak friction angle, the following dilatancy relationship proposed by Bolton (1986) was used:

$$\phi'_p = \phi'_c + AI_R \quad (4)$$

where ϕ'_p = peak friction angle; ϕ'_c = critical-state friction angle; A = 5 and 3 for plane-strain and triaxial conditions, respectively. The dilatancy index I_R is given by:

$$I_R = I_D[10 + \ln(\frac{p_A}{100\sigma'_{mp}})] - 1 \quad (5)$$

where I_D = relative density = D_R(%)/100; p_A = 100 kPa; σ'_{mp} = mean effective stress at peak strength in the same units as p_A. Eqs. (4) and (5) were used to define the non-linear Drucker-Prager failure surface in the finite element analyses.

3.2 *Numerical modeling of multiple footings*

Three different cases of multiple-footing configuration were considered in the finite element analysis. These are shown in Figure 2. Cases 1 and 2 correspond to two and three footings in line, respectively, while case 3 corresponds to a five-footing in two perpendicular directions. For each configuration, different footing distances L_1 and L_2 were used in the analyses.

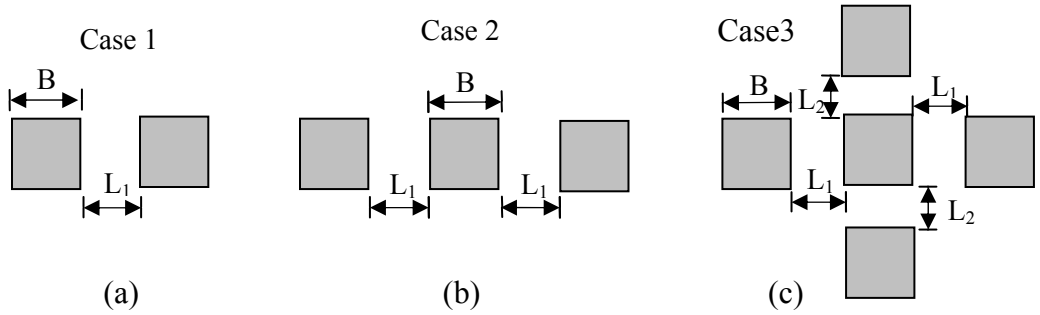

Figure 2. Configuration of multiple footing arrangements in finite element analysis.

The finite element models were constructed using the program ABAQUS with twenty-noded 3D solid elements. The total number of elements for the analysis of a single footing was 12,000. The size of the finite element mesh was 36m (width) × 42m (length) × 21m (depth), while the width of footing (B) was 1.2m. The size of the mesh represents more than 30 and 17 times the footing width laterally and axially, respectively. Boundary conditions were of the fixed and roller types for the bottom and lateral boundaries, respectively. Loads were applied incrementally to the footings. The soils were assumed in all cases to be dense clean silica sand with $\gamma = 15.6$ kN/m^3 and $K_0 = 0.5$. Details on the finite element modeling and soil conditions can also be found in Lee et al. (2008).

4 STRAIN INFLUENCE FACTORS FOR MULTIPLE FOOTINGS

4.1 *Strain influence diagram*

Figure 3 shows depth profiles of strain influence factor I_z for the multiple-footing cases 1, 2, and 3 with different footing distances. In cases 2 and 3, the profiles correspond to those for the center footing. As shown in the figure, the values of I_z down to the depths at which $I_z = I_{zp}$ and the value of I_{zp} itself are nearly constant, irrespective of the distances between the footings and the number of footings considered. The depth to I_{zp} is also fairly constant, at approximately 0.5 B. Values of I_z for the part of the influence zone below the peak in the influence diagram increase as the footing distances decrease. For case 1, no significant variation of I_z values is observed for different footing distance ratios. At a distance ratio $L_1 = 3.0B$, the profile is practically indistinguishable from that for a single footing, indicating that there would be no need to account for the interaction between footings for footing distance ratios L_1/B greater than 3. In the case of the three aligned footings (case 2), it is seen that the I_z profiles are similar to those of the two side-by-side footings (case 1), but the rate of increase of I_z with L_1/B is higher. Similarly to case 1, the effect of footing interaction decreases as the footing distance ratio increases, becoming negligible for distance ratios L_1/B greater than 3. The lack of dependence of I_z values on the distance between footings for the zone above the depth to I_{zp} (observed also in case 1) can be attributed to the fact that load transfer takes place in a direction such that the stress fields caused by each footing separately do not merge for that depth range, even for relatively small spacings.

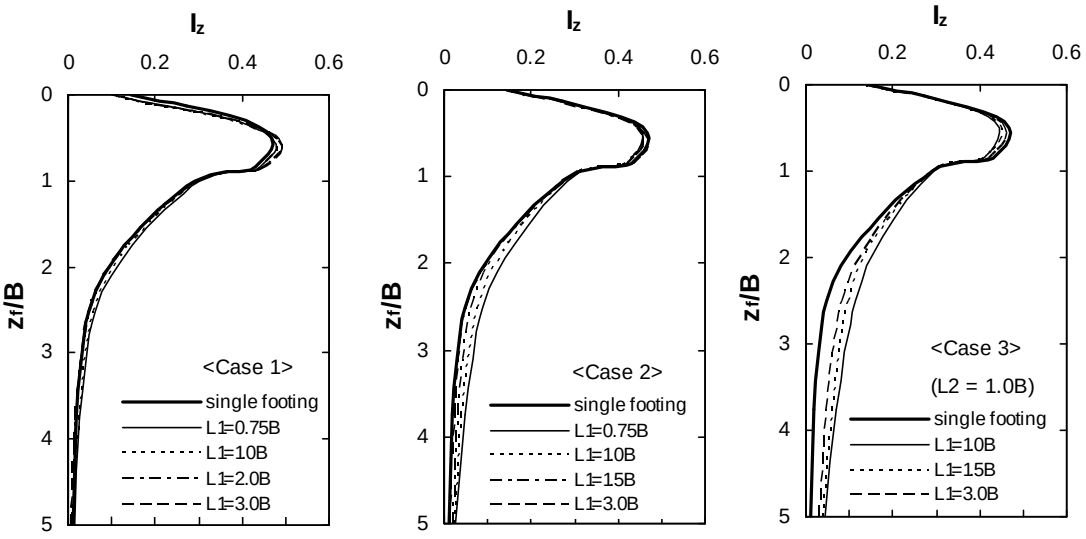

Figure 3. Depth profiles of I_z for cases 1, 2 and 3.

For case 3 in Figure 3c, compared with results for cases 1 and 2, the increase of I_z is found to be quite considerable. Since the variation of I_z values for case 3 results from the combined effects of the two footing distances L_1 and L_2, the minimum values considered in the analysis for L_1/B and L_2/B (both equal to 1) yield the largest increase of I_z values in Figure 3c.

4.2 *Design application*

From this study, it was found that the depth of the strain influence zone (i.e., z_{f0}) is the significant component in the strain influence diagram for multiple footings, which varies according to footing distance. Figure 4 shows values of z_{f0}/B for multiple-footing cases 1, 2 (Fig. 4a) and 3 (Fig. 4b) as a function of the normalized distances L_1/B and L_2/B. For cases 1 and 2 with $L_1/B = 1$, the strain influence depths were 9 % and 15 % larger than the 2B observed for a single footing, respectively. It is also seen that for $L_1/B \geq 3$ the influence on the settlement of a given footing on the adjacent footing or footings is negligible.

For case 3, the strain influence depths also vary as a function of the combined effects of the two distances. When both L_1/B and L_2/B are lager than 3, there is essentially no interaction between the adjacent footings. For multiple footings with footing distance ratios less than 3, the strain influence diagram developed for a single footing must be modified using Figure 4 for the applicable values of the distance ratios L_1/B and L_2/B.

For multiple footings, the key variable that needs to be modified is z_{f0}. Using the results shown in Figure 4, the equations for z_{f0} are:

$$\frac{z_{f0}}{B} = 0.22 \cdot \exp\left[1.1 \cdot \left(0.6 - \frac{L_1}{B}\right)\right] + 2 \qquad \text{for case 1} \qquad (6)$$

$$\frac{z_{f0}}{B} = 0.50 \cdot \exp\left[1.2 \cdot \left(0.6 - \frac{L_1}{B}\right)\right] + 2 \qquad \text{for case 2} \qquad (7)$$

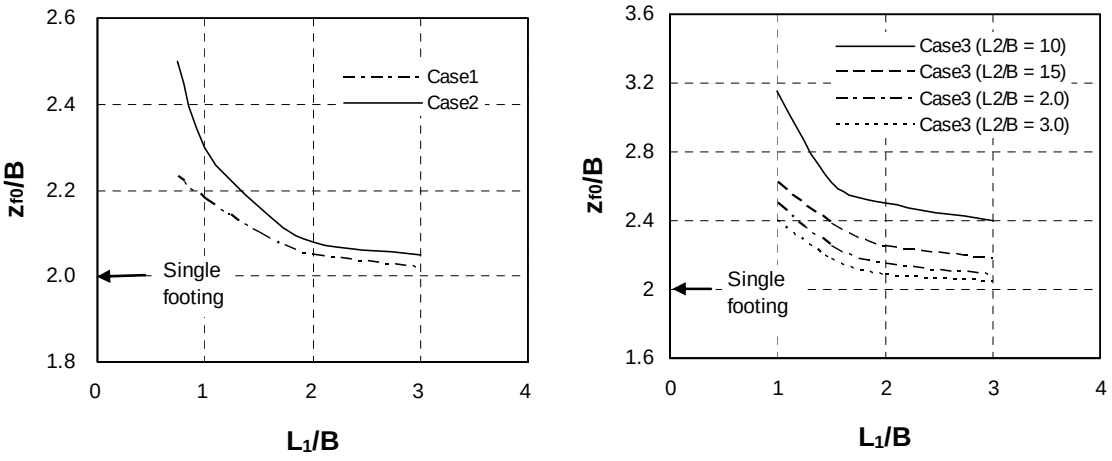

Figure 4. Depth of strain influence zone for cases 1, 2 and 3.

$$\frac{z_{f0}}{B} = 0.83 \cdot \left(\frac{L_2}{B}\right)^{-0.17} \left[0.75 \cdot \exp\left[2 \cdot \left(0.75 - \frac{L_1}{B}\right)\right] + 2\right] \qquad \text{for case 3} \tag{8}$$

Once the footing dimensions and configurations are selected, the strain influence diagram shown in Figure 1 can be reconstructed using z_{f0} calculated from Eqs. (6) to (8).

5 SUMMARY AND CONCULSIONS

Shallow foundations typically consist of multiple footings. Most conventional methods used for the estimation of footing settlement have been developed for an isolated footing, and do not provide a way to account for interaction between adjacent footings. In this paper, a method of settlement estimation that takes account of the proximity of neighboring footing was presented based on Schmertmann's framework. Three-dimensional nonlinear finite element analyses were performed to obtain the load-settlement responses and strain distributions in the foundation soils under multiple footing conditions. Three different arrangements of square footings at different distances were considered in the finite element analyses. The finite element analyses produced values of I_z for two, three and five footings arranged in various ways.

The results of the analyses show that the depth of the strain influence zone in the strain influence diagram needs to be modified to account for the interaction between footings. New strain influence diagrams for multiple footing conditions were presented. These were mainly based on the diagram of Schmertmann's method proposed for a single footing, with corrected depth of the strain influence zone as a function of L_1/B and L_2/B for various multiple footing configurations. Design equations for the influence depths associated with the modified strain influence diagrams obtained from the finite element analyses were presented as well.

6 REFERENCES

Berardi, R., Jamiolkowski, M., and Lancellotta, R. 1991. Settlement of shallow foundations in sands selection of stiffness on the basis of penetration resistance. *Proceedings of the Congress Sponsored by the Geotechnical Engineering Division of the ASCE*, Geotechnical Special Publication 27, 185 – 200.

Bolton, M. D. 1986. The strength and dilatancy of sands. *Geotechnique* 36(1): 65 –78.

Lee, J. and Salgado, R. 1999. Determination of pile base resistance in sands. *Journal of Geotechnical and Geoenvironmental Engineering* 125 (8): 673 - 683.

Lee, J. and Salgado, R. 2002. Estimation of footing settlement in sand. *International Journal of Geomechanics* 2(1): 1 – 28.

Lee, J., Eun, J., Prezzi, M., and Salgado, R. 2008. Strain influence diagrams for settlement estimation of both isolated and multiple footings in sand. *Journal of Geotechnical and Geoenvironmental Engineering* 134(4): 417 - 427.

Meyerhof, G. 1965. Shallow foundations. *Journal of Soil Mechanics and Foundations Division* 91(SM2): 21 – 31.

Schmertmann, J. H. 1970. Static cone to compute static settlement over sand. *Journal of Soil Mechanics and Foundations Division* 96(SM3): 1011 – 1042.

Schmertmann, J. H., Hartman, J. P., and Brown, P. R. 1978. Improved strain influence factor diagrams. *Journal of the Geotechnical Engineering Division* 104(GT8): 1131 – 1135.